

Semiconductor devices

Light-emitting diodes as chemical sensors

Semiconductor devices¹ make good chemical sensors, being responsive, selective and compact. Some gas analytes, for example, can be photometrically detected by the electroluminescence they absorb from semiconductor light-emitting diodes^{2,3}. Here we show that the intensity of this electroluminescence can be modulated in another way entirely, namely as a result of the adsorption of analyte onto the surface of the light-emitting diode, which affects its radiative efficiency by altering its surface-state structure and causes rapid, stable and reversible changes in electroluminescent intensity. Such devices are complementary to existing metal oxide-based resistance sensors, offering the advantages of low-power, room-temperature operation and ready integration into array-based devices.

Light-emitting diodes (LEDs) designed for high optical efficiency employ thin quantum-well active regions^{4,5}. However, the LED-based chemical sensors we describe here are designed to optimize the active layer's surface interactions so that adsorption effects on carrier recombination processes are accentuated. Such chemical adsorption can alter the nature and energy distribution of surface states that affect surface recombination velocity and radiative efficiency^{6,7}.

We used a double-heterostructure LED (Fig. 1a), grown by low-pressure metal-organic chemical vapour deposition. This has a conventional p-type/n-type junction arrangement, consisting of an active layer of undoped In_{0.49}Ga_{0.51}P, and p-type and n-type cladding layers of (Al_{0.5}Ga_{0.5})_{0.51}In_{0.49}P, grown to be lattice-matched to GaAs substrates; a highly doped p-type GaAs contact layer completes the structure. Each cladding layer is 0.5 μm thick and the active-layer thickness was varied from 50 to 500 nm. We processed the LED structures into broad-stripe (500 × 1,000 μm²) devices with cleaved (110) output facets.

The experimental set-up is adapted from semiconductor photoluminescent studies⁸. When forward-biased, the LEDs give red electroluminescence with band maxima at about 670 nm. Packaged devices were operated continuously at low and constant current levels (around 20 mA) to minimize heating and superluminescence. Electroluminescence experiments were carried out in the presence of five optically transparent analyte gases: ammonia (NH₃), methylamine (NH₂CH₃), dimethylamine (NH(CH₃)₂), trimethylamine (N(CH₃)₃) and sulphur dioxide (SO₂). A vacuum (10⁻³ torr) served as the reference ambient.

Figure 1b shows a typical trace of electroluminescence intensity against time for a

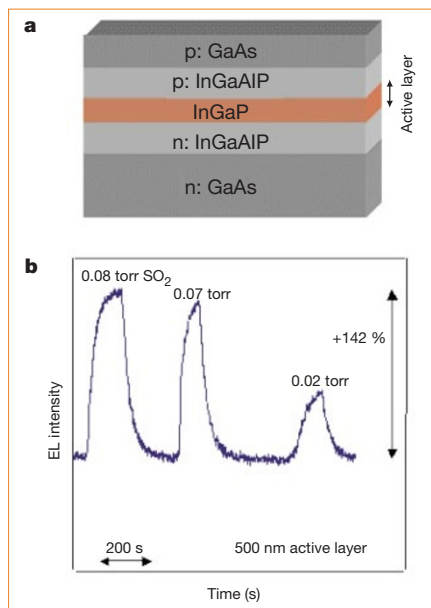


Figure 1 Diode structure and the response of its electroluminescence to sulphur dioxide. **a**, Double heterostructure p-n junction diode. Electrical contact is made to the top and bottom surfaces with metal films (layer dimensions not drawn to scale). **b**, Changes in electroluminescence intensity at 670 nm of a double-heterostructure diode upon exposure to SO₂ gas, relative to a vacuum ambient. The partial pressure of SO₂ is indicated; the sample is returned to the vacuum ambient between each exposure.

LED exposed to SO₂. Enhancement increases with active-layer thickness, reaching several hundred per cent for the double heterostructures with the thickest active layer. The reversible responses (Fig. 1b) demonstrate the potential for online sensing with these structures. All of the analyte-diode structure combinations displayed adsorption and desorption times of less than a few minutes at room temperature. For all analytes, enhancements are seen at pressures as low as about 0.01 torr, with the response saturating at around 0.1–1 torr. The electroluminescent response is reproducible even after weeks of storage in air.

This adsorbate-induced modulation of electroluminescent intensity from simple double-heterostructure diodes illustrates their application as transducers that can couple semiconductor surface chemistry to an optical signal. The remarkable features of these structures (robust, inexpensive, small, low power consumption, compositionally tunable emission spectra) could allow arrays to be used to identify a variety of analytes. Highly sensitive, ultrasmall LEDs with large surface-to-volume ratios should then be easily integrated with diodes that serve as photodetectors, forming monolithic chemical sensors. From photoluminescent studies of semiconductors^{6,9,10} and from electroluminescence of molecular diodes¹¹, it should be possible to customize the selectivity, sensitivity and speed of the electroluminescent response by surface modification.

Albena Ivanisevic*, Jeng-Ya Yeh†, Luke

Mawst†, Thomas F. Kuech‡, Arthur B. Ellis*
Departments of *Chemistry, †Electrical and Computer Engineering and ‡Chemical Engineering, University of Wisconsin, Madison, Wisconsin 53706, USA

- Janata, J. & Josowicz, M. *Acc. Chem. Res.* **31**, 241–248 (1998).
- Krier, A., Sherstnev, V. V. & Gao, H. H. *J. Phys. D* **33**, 1656–1661 (2000).
- Ohyama, T. *et al. Sensors and Actuators B* **64**, 142–146 (2000).
- Ponce, F. A. & Bour, D. P. *Nature* **386**, 351–359 (1997).
- Stringfellow, G. B. in *High Brightness Light Emitting Diodes* Vol. 48 (eds Stringfellow, G. B. *et al.*) 1–45 (Academic, New York, 1997).
- Seker, F., Meeker, K., Kuech, T. F. & Ellis, A. B. *Chem. Rev.* **100**, 2505–2536 (2000).
- Boroditsky, M. *et al. J. Appl. Phys.* **87**, 3497–3504 (2000).
- Lorenz, J. K., Kuech, T. F. & Ellis, A. B. *Langmuir* **14**, 1680–1683 (1998).
- Kelly, M. T., Chun, J. K. M. & Bocarsly, A. B. *Nature* **382**, 214–215 (1996).
- Harper, J. & Sailor, M. J. *Anal. Chem.* **68**, 3713–3717 (1996).
- Kunugi, Y. *et al. Chem. Mater.* **10**, 1487–1489 (1998).

Public health

Screening slaughtered cattle for BSE

The systematic testing of slaughtered cattle aged over 30 months, or alternatively their elimination from the food chain, is an important component of a package of measures introduced in the European Union on 1 January 2001 to combat bovine spongiform encephalopathy (BSE) and protect human health. Here we explore the analytical limit of a rapid test designed to detect the abnormal prion protein associated with BSE in bovine brain and find that it is comparable to the limit of detection of infectivity in the conventional mouse bioassay¹, which is impractical for systematic screening. The sensitivity of the biochemical test allows it to be used as a viable alternative to the destruction of all carcasses of cattle slaughtered after 30 months of age. Additional work is required to compare this analytical sensitivity with the diagnostic sensitivity of the test under conditions of routine post-mortem BSE diagnosis and surveillance.

In May 1999, the European Commission evaluated four tests² based on the detection of PrP^{Res} (also known as PrP^{Sc}), the abnormal protease-resistant form of the prion protein that is the only known molecular marker for BSE and related prion disorders. We have used a commercial version of the most analytically sensitive of these four tests (Bio-Rad version of the CEA test 'D') on serial dilutions of three samples taken from an undiluted homogenate of brainstem material pooled from several BSE cases and previously assayed for infectivity by titration in mice. The results in Fig. 1a show good agreement between the triplicate samples and a limit to detection of the absorbance signal in the assay at a 1/1,000 dilution of the infected brain homogenate.

In the mouse bioassay, the infectivity

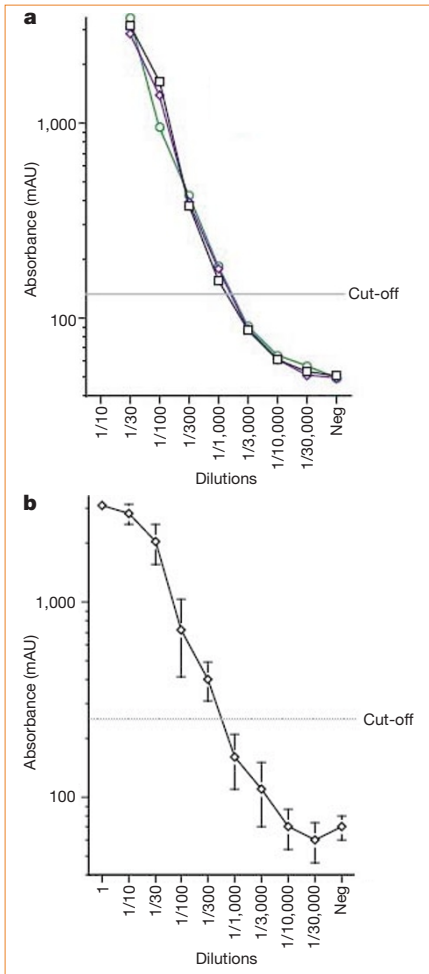


Figure 1 Testing *in vitro* for protease-resistant prion protein (PrP^{res}) in BSE-infected brain tissue. **a**, Triplicate samples from pooled infected brainstem homogenate were assayed using a commercial BSE-testing kit (Bio-Rad) based on sandwich immunoassay of rapidly purified PrP^{res} by enzyme-linked immunosorbent assay (ELISA)^{2,3}. Samples were rehomogenized at 20% w/v in the buffer of the Bio-Rad purification kit. Serial dilutions were made using a pool of 20% w/v BSE-negative brain homogenate prepared in the same conditions. Testing was performed according to the manufacturer's indications. The equivalent of 33 mg of brain was loaded in each ELISA well. We used the absorbance limit recommended by the manufacturer (defined as the background absorbance of the ELISA buffer R3 + 0.090 absorbance units (AU) = 0.133 AU) to determine the cut-off sensitivity of the test. All dilutions up to 1/1,000 were above the cut-off for all three samples. The signal detected at the 1/3,000 dilution was below the recommended cut-off. The titre of the inoculum was 10^{3.3} LD₅₀ g⁻¹, or 66 LD₅₀ units per 33 mg of brain (equivalent to the amount loaded in one ELISA well); the dilution 1/1,000 corresponds to 0.066 LD₅₀ units per ELISA well. 'Neg' indicates normal bovine brain material. **b**, PrP detection in diluted homogenates tested under blind conditions during the EC evaluation of May 1999 (20 samples per dilution; errors bars correspond to standard deviation)¹⁻³. The commercial kit used in **a** employs the enzyme peroxidase, which gives a lower R3 background absorbance than the acetylcholinesterase used in the earlier tests. The sensitivity cut-off here is therefore higher (0.250 AU), corresponding to 2.5 times the mean of the negative samples analysed (2.5 × 100 mAU = 250 mAU). This cut-off was consistent with a 100% specificity on a series of 1,064 negative bovine samples from New Zealand; 18/20 homogenates were detected as positive at a dilution of 1/300, and 1/20 at a dilution of 1/1,000 with this homogenate¹ (infectivity 10^{3.1} LD₅₀ g⁻¹, or 35 LD₅₀ per 28 mg of brain (equivalent to the amount loaded in one ELISA well); the 1/300 dilution corresponds to the equivalent of 0.1 LD₅₀ per ELISA well).

titre of the reference material inoculated into mice was 1 LD₅₀ unit per 0.5 mg infected bovine brain (where the dose corresponding to one LD₅₀ unit has a 50% chance of killing the mouse); the limit of detection of the biochemical test corresponds to 0.033 mg of this BSE-positive bovine brain material (Fig. 1, legend). Direct comparison with results from titration in mice (Table 1) shows that the highest dilution of material for which infection can be detected in the

bioassay also gives a positive result in the biochemical test (1/1,000; 3 of 3 samples positive). The limit of detection of the test is therefore well below 1 LD₅₀ unit in mice. This is a critical finding because most information on infectivity refers to data from this conventional mouse model, although the sensitivity of detection of infectivity should be improved as transgenic mouse models become available.

The calibration curves shown in Fig. 1a

are consistent with results obtained using different diluted homogenates of similar infectivity and tested blind during early evaluation by the European Commission²⁻⁴ (Fig. 1b). This provides an indication of the reproducibility of this PrP^{res} detection test and suggests a direct relationship between infectivity titre and PrP^{res} concentration.

The relevance of making serial dilutions to evaluate the sensitivity has been confirmed on preclinical samples containing various concentrations of BSE agent using central nervous system tissue obtained in a pathogenesis study conducted in the United Kingdom⁵ (our unpublished results).

Our results show that this PrP^{res}-detection test on brain material offers a level of assurance regarding the detection of the presence of infection that is at least comparable with that provided by the conventional mouse bioassay. Although bovines are regarded as the most sensitive recipient species for BSE, the oral route in cattle is less efficient in establishing infection with the BSE agent than is direct injection into mouse brain: the differential factor is currently estimated¹ at around 100 (on the grounds that 1 g brain titrating 10^{3.3} LD₅₀ g⁻¹ can theoretically kill, with a probability of 50%, 2,000 mice injected intracerebrally or 20 bovines contaminated orally). It is reasonable to presume that humans contaminated by the oral route are partially protected by the species barrier and so are less sensitive than cattle to the BSE agent (although this differential factor is not known). Consequently, risk assessment generally assumes that humans contaminated by the oral route are less sensitive to the BSE agent than mice inoculated intracerebrally.

Routine application of the test should help eliminate previously undiagnosed BSE-affected animals from the food chain and provide tighter epidemiological monitoring of the BSE epidemic.

J. P. Deslys*, E. Comoy*†, S. Hawkins‡, S. Simon§, H. Schimmel||, G. Wells‡, J. Grassi§, J. Moynagh¶

*CEA, Service de Neurovirologie, DRM/DSV, BP6 92265 Fontenay-aux-Roses, France
e-mail: jpdesslys@cea.fr

†Bio-Rad Life Sciences Laboratories, Hercules, California 94547, USA, and Marnes-la-Coquette 92430, France

‡Veterinary Laboratories Agency, New Haw, Addlestone, Surrey KT15 3NB, UK

§CEA, Service de Pharmacologie et d'Immunologie, DRM/DSV, Saclay, France

||Joint Research Centre, Institute for Reference Materials and Measurements, Retieseweg, B2440 Geel, Belgium

¶Directorate General Health and Consumer Protection, European Commission, Rue Belliard 232, 1049 Bruxelles, Belgium

1. European Commission in Oral Exposure of Humans to the BSE Agent: Infective Dose and Species Barrier 31 (Scientific Steering Committee meeting, 13-14 April 2000).
2. Moynagh, J. & Schimmel, H. *Nature* **400**, 105 (1999).

Table 1 ELISA detection of PrP^{res}

Dilution	PrP ^{res} detection			Infectivity (dead/total)
	Sample 1	Sample 2	Sample 3	
1/10				17/18
1/30	3,166	2,880	3,466	
1/100	1,618	1,318	958	15/17
1/300	378	396	429	
1/1,000	155	179	186	1/14
1/3,000	87	88	91	
1/10,000	61	61	64	0/7
1/30,000	53	51	57	
1/100,000	-	-	-	0/9
Neg	51	49	49	NT
ELISA buffer	43	43	43	
Cut-off	133	133	133	

Absorbance values for each sample correspond to those shown in Fig. 1a. To determine infectivity, reference BSE-infected brain homogenate was titrated in Rlll mice. Serial dilutions of brain were prepared and each of 20 mice per group was inoculated with a single dilution (20 µl by intracerebral route + 100 µl by intraperitoneal route per animal). Results are expressed as the number of mice developing the disease/number of mice surviving at the time when the first mouse developed the disease. (The denominator of the incidence of mice succumbing to disease is corrected to eliminate mice lost to the assay before the minimum incubation period started at which they could have developed disease; in groups where no infectivity was detected, the denominator is expressed as the number of mice surviving to the completion of the assay at 700 days.) NT, not tested. Neg, normal bovine brain.

- European Commission *The Evaluation of Tests for the Diagnosis of Transmissible Spongiform Encephalopathy in Bovines* (http://europa.eu.int/comm/food/fs/bse/bse12_en.html).
- Grassi, J. *et al. Arch. Virol.* **16** (suppl.), 197–205 (2000).
- Wells, G. A. H. *et al. Vet. Rec.* **142**, 103–106 (1998).

Genome evolution

Gene capture in archaeal chromosomes

Free genetic elements can be readily integrated into bacterial chromosomes, but so far, with the exception of one virus, there has been no evidence that this happens in Archaea — the other domain of microorganisms. Here we show that site-specific integration of different genetic elements into archaeal chromosomes is a general phenomenon, albeit rare, which requires an archaeal integrase and produces a partitioned integrase gene in the chromosome. The process is distinct from bacterial mechanisms and has implications for how horizontal gene transfer might occur across the boundaries of the domains of life.

Many bacterial integrases belong to a superfamily of tyrosine recombinase enzymes¹ and mediate site-specific recombination between small extra-chromosomal DNA elements and chromosomes², facilitating horizontal gene transfer between bacteria². The only known archaeal integrase effects site-specific and reversible integration of the SSV1 virus into the chromosome of *Sulfolobus shibatae*^{3,4} (Fig. 1a, top).

We have previously identified a region of the *Sulfolobus solfataricus* genome that shows high sequence similarity to the *Sulfolobus* plasmid pHEN7 and to other members of the pRN plasmid family^{5–7}. This chromosomal region is flanked by open-reading

frames (ORFs) with extensive sequence similarity to the amino-terminal (66 amino acids) and carboxy-terminal (269 amino acids) regions of the SSV1 integrase (Fig. 1a). The former, Int(N), overlaps with the downstream half of a gene encoding tRNA^{Val} and shows 71% sequence identity to the 45-base-pair target site (*att*) of the SSV1 integrase⁴ (within the downstream half of a tRNA^{Arg} gene), whereas the latter, Int(C), contains an identical *att* site (Fig. 1a, b).

Excision from the chromosome by recombination at the direct *att* repeat and circularization creates a plasmid, pXQ1, containing an intact integrase gene and one copy of the *att* site, similar to that of the SSV1 virus⁴. Thus, with the aid of the encoded integrase, pXQ1 could have integrated into the chromosome. As neither the free form of pXQ1 nor the empty chromosomal site of *Sulfolobus* were detectable by polymerase chain reaction (our unpublished results), we infer that the absence of an intact integrase gene precludes integrase-mediated excision from the chromosome.

A search for more homologues of the SSV1 integrase encoded in the chromosome of *S. solfataricus*⁵ revealed three Int(N)s and one Int(C). The sequences encoding Int(N) overlap with downstream halves of tRNA genes and all the sequences contain *att* sites. By analogy to the SSV1 virus, a genetic element XQ2 (67.7 kilobases) can be formed by recombination and excision at the *attL* and *attR* sites (Fig. 1a, b).

Four of the ORFs encoded in XQ2 were assigned to genes encoding the enzymes dTDP–glucose-4,6-dehydratase, glucose-1-phosphate–thymidyl transferase, dTDP–4-dehydrorhamnose reductase and dTDP–4-dehydrorhamnose-3,5-epimerase, all of which are involved in central metabolism,

and three of which are generally clustered in one operon. However, there are two additional copies of dTDP–glucose-4,6-dehydratase and another copy of each of the other enzymes encoded within the *S. solfataricus* chromosome⁵ that show 76–84% sequence identity and 86–96% similarity. It is therefore likely that XQ2 entered the chromosome, aided by its own integrase, to produce a gene-capture event.

We searched the complete genome sequences of seven other archaea for integrase homologues⁸. Those from the euryarchaeote *Pyrococcus horikoshii*⁹ and the crenarchaeote *Aeropyrum pernix*¹⁰ each had two Int(N), overlapping downstream halves of tRNA genes, and two and one copy of Int(C), respectively. The genome of *Pyrococcus* OT3 has two partitioned integrase genes¹¹. Complementary fragments of the integrase genes contain *att* sites and border regions of 21.5 and 4 kilobases in *P. horikoshii* and 17.5 kilobases in *A. pernix*. Compatible with the idea that these are inserts from unknown organisms, none of their ORFs reveals any hits in the GenBank/EMBL databases⁸. We have detected a total of seven partitioned integrase genes, on average one per genome. Their sequences vary markedly in the amino-terminal region but are less variable in the carboxy-terminal region (22–33%/41–51% identity/similarity), indicating that other integrase genes may still remain to be discovered.

We conclude that chromosomal integration in archaea differs from that in bacteria in producing partitioned integrase genes and that integration can be reversed only if the intact integrase is produced⁴. ‘Curing’ the cell of the free genetic element carrying the intact integrase gene can thus lead to gene capture by the archaeal chromosome. Although archaeal integrases differ from bacterial integrases in lacking a conserved motif¹ and in having *att* sites in the coding region, they may still facilitate gene transfer between archaea, bacteria and eukaryotes¹².

Qunxin She*, Xu Peng*, Wolfram Zillig†, Roger A. Garrett*

*Microbial Genome Group, Institute of Molecular Biology, University of Copenhagen, Sølvgade 83H, DK-1307 Copenhagen K, Denmark

†Max-Planck-Institut für Biochemie, D-82152 Martinsried, Germany

- Nunes-Düby, S. E. *et al. Nucleic Acids Res.* **26**, 391–406 (1998).
- Rowe-Magnus, D. A. & Mazel, D. *Curr. Opin. Microbiol.* **2**, 483–488 (1999).
- Reiter, W.-D. & Palm, P. *Mol. Gen. Genet.* **221**, 65–71 (1990).
- Muskhelishvili, G., Palm, P. & Zillig, W. *Mol. Gen. Genet.* **237**, 334–342 (1993).
- She, Q. *et al. DNA Sequence* **11**, 183–192 (2000).
- Kletzin, A., Lieke, A., Ulrich, T., Charlebois, R. L. & Sensen, C. W. *Genetics* **152**, 1307–1314 (1999).
- Peng, X., Holz, I., Zillig, W., Garrett, R. A. & She, Q. *J. Mol. Biol.* **303**, 449–454 (2000).
- Altschul, S. F. *et al. Nucleic Acids Res.* **25**, 3389–3402 (1997).
- Kawarabayasi, Y. *et al. DNA Res.* **5**, 55–76 (1998).
- Kawarabayasi, Y. *et al. DNA Res.* **6**, 83–101 (1999).
- Makino, S., Amano, N., Koike, H. & Suzuki, M. *Proc. Jpn. Acad. Ser. B* **75**, 166–171 (1999).
- Groth, A. C., Olivares, E. C., Thyagarajan, B. & Calos, M. P. *Proc. Natl Acad. Sci. USA* **97**, 5995–6000 (2000).

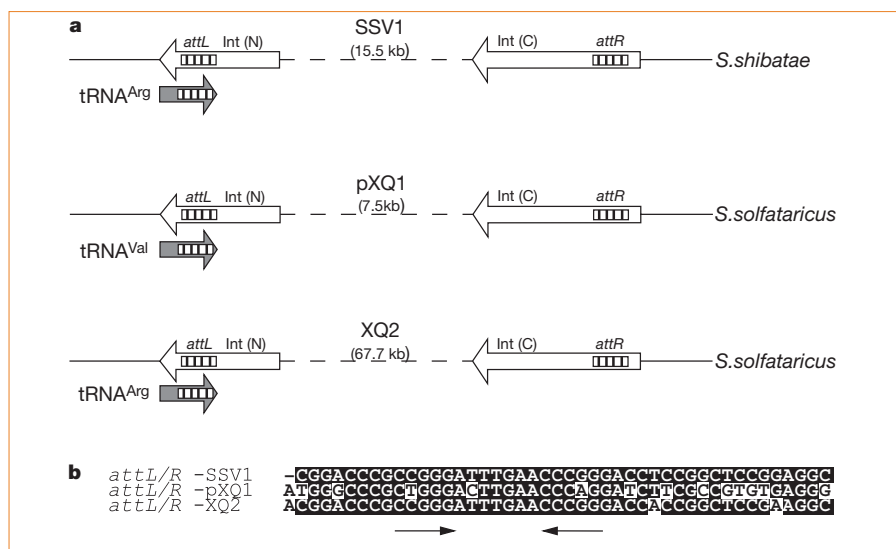


Figure 1 Site-specific integration of genetic elements into archaeal chromosomes. **a**, Organization of the SSV1 virus and the putative genetic elements pXQ1 and XQ2 in the chromosomes of *S. shibatae* and *S. solfataricus*. The relative positions of the partitioned integrase genes, the *att* sites (45 base pairs) and the overlapping tRNA genes are indicated. **b**, Alignment of the direct repeats *attL* and *attR* from virus SSV1 and from pXQ1 and XQ2. Nucleotides are shaded if two or more positions are identical. Arrows indicate a 5-base-pair inverted repeat.